Acta Astronautica 195 (2022) 405–415

Contents lists available at ScienceDirect

Acta Astronautica

journal homepage: www.elsevier.com/locate/actaastro

Research paper

Dynamics of rotating tethered system for active debris removal☆

Valeriy Trushlyakov[1], Vadim Yudintsev *,[2]

Omsk State Technical University, 11, pr. Mira, Omsk, 644050, Russia

ARTICLE INFO

Keywords:
Debris
Space tether
Rotation
Longitudinal oscillations
Space tug

ABSTRACT

The motion of a rotating tethered system for active debris removal is considered. The system consists of the space tug and space debris object connected by the tether. The influence of the relative tug–debris orbital motion on the longitudinal oscillations of the tether is investigated. Linearized equations of the tether oscillations are derived, and the estimation of maximum tether deformation is obtained as a function of initial conditions of tug–debris relative motion. An algorithm for the formation of an interception orbit is proposed to minimize the maximum deformation of the tether after the formation of the rotating tether system. The linearized model of longitudinal oscillations is validated by comparing its results with the results of the model of the motion of two bodies connected by a tether in a gravitational field. A numerical example illustrates the obtained results.

1. Introduction

There are a lot of researches is devoted to developing methods for capturing and removing space debris objects [1–6]. Most active debris removal (ADR) methods do not allow using the existing upper stages of launch vehicles (like Fregat, Briz) for ADR tasks. For example, many researchers suggest using tethered towing of the large space debris (SD) objects [7–11] utilizing space tether system (STS). This scheme assumes capturing of the SD using a net [5], harpoon [12] or an autonomous docking module (ADM) [13]. After forming the tethered connection with the debris, the ST tows the SD pulling the tether. This scheme supposes that the tether is fixed in the aft part of the ST, where the propulsion system is located on the existing upper stages. Therefore, the existing upper stages are almost impossible to adapt for ADR by tethered towing (Fig. 1).

Considering the high cost of developing a space system for ADR missions, it is advisable to use such ADR methods, that allow to use existing upper stages of the launch vehicles with minimal modifications. In [14], an alternative tethered towing scheme is proposed using a push towing scheme. The push towing scheme involves the application of the tug's thrust in the direction of the SD, which does not allow the use of a flexible connection between the SD object and the ST. In [14], after the formation of the STS, it is supposed to impart rotation to the system, which leads to stretching the tether and allow to apply the tug thrust

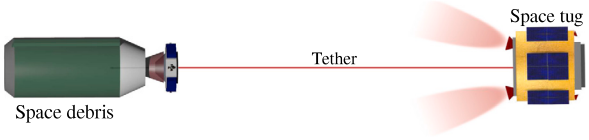

Fig. 1. Pulling space debris object by a tether.

along the tether (Fig. 2). The rotation of the STS can be provided by the tug–debris relative motion before the formation of the STS. The initial angular rate of the rotating STS (RSTS) and its further motion will be determined by the distance between the ST and SD at the moment of the formation of the RSTS, by the relative velocity, by the mass of the ST and SD, and by the tether stiffness. The formation of the RSTS is the moment when the tether starts to strain due to the relative motion of the space tug and debris.

The tethered connection between the ST and SD can be established using the ADM, separated from the ST with the tether [13,15]. The ADM is a small spacecraft that carries all specific equipment for ADR missions, including a gripping device, tether control system, and propulsion system for proximity operations. The use of the ADM will make it possible to simplify the adaptation of existing upper stages for using them as space tugs to solve the problem of ADR, since all new

☆ This document is the results of the research project funded by the Omsk State Technical University.
* Corresponding author.
E-mail addresses: vatrushlyakov@yandex.ru (V. Trushlyakov), yudintsev@classmech.ru (V. Yudintsev).
URL: https://www.classmech.ru (V. Yudintsev).
[1] Professor, Department of Aircraft and Rocket Engineering.
[2] Associate Professor, Senior Researcher at Research and Educational Center "Space Ecology".

https://doi.org/10.1016/j.actaastro.2022.03.023
Received 11 January 2022; Received in revised form 8 March 2022; Accepted 17 March 2022
Available online 26 March 2022

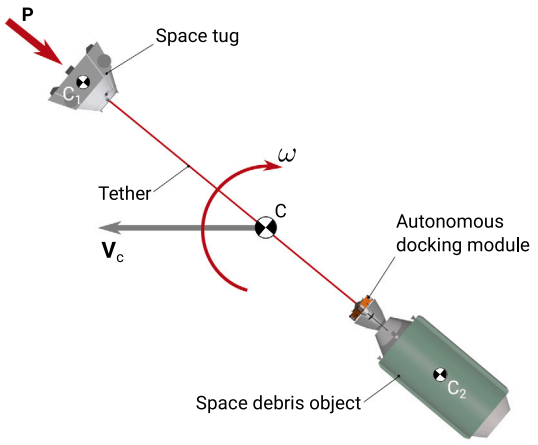

Fig. 2. Rotating space tether system.

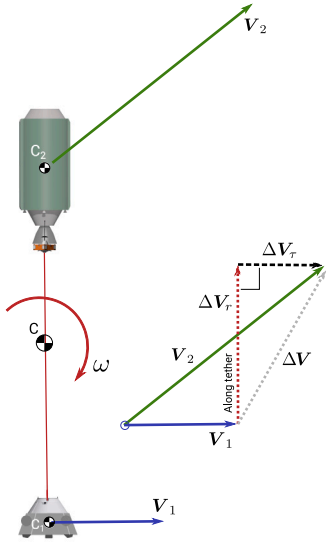

Fig. 3. Relative velocities ΔV_τ and ΔV_r.

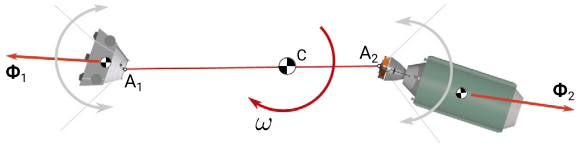

Fig. 4. Oscillations of the ST and SD relative to the tether.

tasks (rendezvous, capture of debris), for which the upper stages is not designed, are delegated to the ADM.

In [14], the equations of motion of a RSTS were obtained and the estimates of the deformation of the tether were given for ideal conditions of the RSTS formation, when the vector difference between the orbital velocities of the ST and SD is perpendicular to the tether line. Obviously, in natural conditions, it is impossible to rely on ideal conditions for the formation of the tethered system due to the inevitable errors in placing the tug into the interception orbit, errors in determining the trajectory of the debris. A more detailed analysis of the STS motion under imperfect conditions of its formation is necessary, and the presented article is devoted to this issue.

2. Statement of the problem

Let us consider a motion of the RSTS consisting of the ST and the SD connected by the massless tether. We suppose that the ST and SD orbit in the same orbital plane. The motion of the system is considered after the moment of establishing the tethered connection between the bodies when the tether starts straining. At that moment, the ST and SD have the velocities $\vec{V}_1$ and $\vec{V}_2$ relative to the Earth-centered inertial frame. The system's motion consists of the center of mass (C) motion, the rotation relative to the center of mass, and the longitudinal oscillation of the tether. The rotation of the system depends on the projection of the velocity difference ($\Delta\vec{V} = \vec{V}_2 - \vec{V}_1$) on the transversal direction of the tether $\Delta\vec{V}_\tau$ and the initial tether length l_0. The longitudinal oscillations of the tether depend on the projection of the velocity difference on the longitudinal direction of the tether $\Delta\vec{V}_r$ and $\Delta\vec{V}_\tau$ (Fig. 3).

It is essential to understand how these velocities affect the tether's deformation or the tension force, which is limited by the strength of the material of the tether. It is also important to develop a method for forming the interception orbit that the ST should follow to minimize tether deformation after the formation of the RSTS. So, the rest of the paper is devoted to (1) investigating the influence of the initial conditions of the RSTS on the longitudinal oscillations of the tether; (2) providing the algorithm of construction the interception orbit of the ST that minimize the amplitude of the longitudinal oscillations of the tether.

Fig. 3 shows an ideal gripping configuration when the longitudinal axes of the SD and ST are aligned with the tether line. The required orientation of the ST relative to the tether could be provided by the control system of the ST, and the attached ADM could provide the required orientation of the SD. But even under these conditions, the longitudinal oscillations of the tether, together with its rotation, will lead to the oscillation of the SD and ST relative to the tether line due to the centrifugal ($\boldsymbol{\Phi}_1$, $\boldsymbol{\Phi}_2$) and Coriolis inertial forces (Fig. 4). The attitude motions of the space tug and debris object relative to the tether will affect the longitudinal oscillation of the tether and vice versa.

To avoid build-up of the SD and ST oscillations relative to the tether line after the formation of the RSTS the control system of the ST should damp the longitudinal oscillation of the tether.

The rest of the paper is organized as follows. In Section 3, the linearized motion equation of longitudinal oscillations of the RSTS is derived, allowing us to obtain an expression for the maximum deformation of the tether. Section 4 discusses the algorithm for intercepting the SD object using ADM separated from the ST. Section 5 provides numerical example that also shows the influence of the tether longitudinal oscillation on the attitude motion of the passive SD object and vice versa.

3. Model

3.1. Motion equations

The model of RSTS is built with the following assumptions: the ST and SD are point masses; the masses of the space tug, debris; the tether is a massless viscoelastic spring. We neglect the effect of the Earth gravity to the tether rotation. Further, it will be shown that the angular velocity of the RSTS must be at least

$$\omega > \sqrt{\frac{P}{m_1 l_0}} \tag{1}$$

where P is the tug's thrust force, m_1 is the mass of the ST, and l_0 is the tether length. For the ST mass about of 10^3 kg, tether length of 1 km, and the tug's thrust at least 1 kN, angular velocity of the STS should be greater than 1.47 deg/s. That angular velocity is much greater than the angular velocity of the STS center of mass orbital motion (mean motion)

$$\omega > \sqrt{\frac{P}{m_1 l_0}} \gg n = \sqrt{\frac{\mu}{a^3}} \tag{2}$$

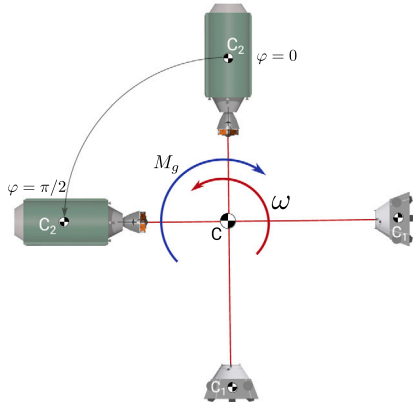

Fig. 5. For comparison of the kinetic energy and the work of gravitational torque.

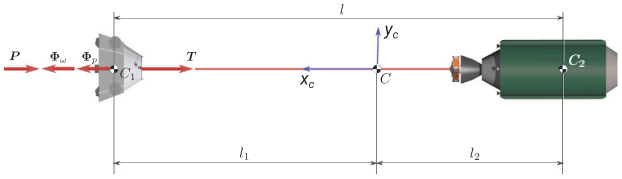

Fig. 6. Scheme of the system.

where μ is the gravitational parameter of the Earth, a is the semimajor axis of the RSTS object orbit. This makes it possible to exclude from consideration the influence of the gravitational torque on the STS motion. Indeed, the rotational kinetic energy of the RSTS is

$$T_r = \frac{1}{2} J_z \omega^2 \tag{3}$$

And the work of the gravitational torque when rotating from $\varphi = 0$ to $\varphi = \pi/2$ (Fig. 5) position is

$$A_g = -\frac{3}{2} J_z n^2 \tag{4}$$

where J_z is the moment of inertia of the STS relative to the center of mass. The kinetic energy to the work ratio is

$$\frac{T_r}{|A_g|} = \frac{1}{3}\left(\frac{\omega}{n}\right)^2 \tag{5}$$

For the circular orbit of the RSTS with the height of 800 km $n \approx 0.001$ rad/s, that ratio is about 219. Therefore, the gravitational torque slightly affects the motion of the RSTS, and we can neglect that effect. In Section 5 the effect of gravitational field of the Earth to the motion of the RSTS are illustrated by numerical example.

The STS starts rotating when the length of the tether equals its free length l_0, and the angular velocity of the system equals to ω_0

$$l(0) = l_0, \quad \omega(0) = \omega_0 \tag{6}$$

The longitudinal oscillation of the system is considered relative to the non-inertial frame. The origin of the frame is placed in the center of mass of the system (C point). The space tug motion along the tether line is described by the equation [14] (Fig. 6)

$$m_1 \ddot{l}_1 = -T - P + \Phi_\omega + \Phi_p \tag{7}$$

In the right side of the equation are the tether tension force T, tug's thrust P, and two inertial forces caused by the acceleration of the center of mass of the system (Φ_p), and the rotation of the tether (Φ_ω). The tether tension force T depends on the tether stiffness ($c = EA/l_0$) and damping properties of the tether. We suppose that tether tension force is proportional to the deformation $\delta = l - l_0$ and deformation velocity $\dot{\delta} = \dot{l}$

$$T = c\delta + k_d \dot{l} \tag{8}$$

where E is the Young's modulus of the tether, A is the cross sectional area of the tether, k_d is the damping coefficient. Additional terms Φ_ω, Φ_p that address non-inertial properties of the frame $Cx_cy_cz_c$ are

$$\Phi_\omega = \omega^2 l_1 m_1, \quad \Phi_p = \frac{P}{m_1 + m_2} m_1 \tag{9}$$

The distance from the center of mass of the system to the center of mass of the ST can be expressed as

$$l_1 = \frac{m_2}{m_1 + m_2}(l_0 + \delta) \tag{10}$$

Substituting (8)–(10) into (7) we get

$$\ddot{\delta} = -\frac{EA}{l_0 m_{12}}\delta - \frac{k_d}{m_{12}}\dot{\delta} + \omega^2(l_0 + \delta) - \frac{P}{m_1} \tag{11}$$

where m_{12} is the reduced mass of the system

$$m_{12} = \frac{m_1 m_2}{m_1 + m_2} \tag{12}$$

Let us denote the squared natural frequency of the longitudinal tether oscillation as

$$k^2 = \frac{EA}{m_{12} l_0}, \tag{13}$$

and the damping coefficient

$$\eta = \frac{k_d}{m_{12}} \tag{14}$$

and represent the tether deformation δ as product of unit deformation and free length of the tether $\delta = \varepsilon l_0$. The equation of longitudinal oscillations of the tether gets the form

$$\ddot{\varepsilon} + k^2\varepsilon + 2\eta\dot{\varepsilon} = \omega^2(1 + \varepsilon) - \frac{P}{m_1 l_0} \tag{15}$$

This equation is non-linear due to the dependence of ω on the unit length deformation ε. Eq. (15) has the stationary solution ($\dot{\varepsilon} = \ddot{\varepsilon} = 0$)

$$\varepsilon_s = \frac{\omega_s^2 - \frac{P}{m_1 l_0}}{k^2 - \omega_s^2} \tag{16}$$

from which one can obtain stationary unit deformation of the tether ε_s for given stationary angular velocity ω_s. For $\varepsilon_s > 0$ the tug's thrust should obey

$$P < \omega_s^2 m_1 l_0 \quad or \quad \omega_s > \sqrt{\frac{P}{m_1 l_0}} \tag{17}$$

This expression can be used to obtain the minimum angular velocity of the STS for a given tug's thrust.

In the absence of the external torques, the angular velocity ω of the tethered–tug–debris system depends on the tether length and the initial momentum of the system relative to the center of mass

$$K_r = \left(l_1^2 m_1 + l_2^2 m_2\right)\omega = m_{12} l^2 \omega = \text{const} \tag{18}$$

Let us suppose that at the moment of the formation of the STS, the length of the tether was equal to its free length l_0. In this case the initial angular velocity of the tethered system will be determined by the expression

$$\omega_0 = \frac{\Delta V_\tau}{l_0} = \frac{\left|\left(\vec{V}_2 - \vec{V}_1\right) - \vec{e}_r\left[\left(\vec{V}_2 - \vec{V}_1\right)\cdot\vec{e}_r\right]\right|}{l_0} \tag{19}$$

where $\vec{e}_r$ is the unit vector of the tether line

$$\vec{e}_r = \frac{\vec{r}_2 - \vec{r}_1}{|\vec{r}_2 - \vec{r}_1|} \tag{20}$$

From the moment of the formation of the rotating STS, the tether will begin to strain, which leads to a decrease in its angular velocity. It follows from (18) that

$$\omega = \frac{l_0^2}{l^2}\omega_0 = \frac{1}{(1+\varepsilon)^2}\omega_0 \tag{21}$$

Substituting (21) into (15) we get

$$\ddot{\varepsilon} + k^2\varepsilon + 2\eta\ \dot{\varepsilon} = \frac{\omega_0^2}{(1+\varepsilon)^3} - \frac{P}{m_1 l_0} \tag{22}$$

For $\varepsilon \ll 1$ we can linearize the first term in the right side

$$\frac{1}{(1+\varepsilon)^3} \approx 1 - 3\varepsilon \tag{23}$$

and rewrite the (22) as

$$\ddot{\varepsilon} + \left(k^2 + 3\omega_0^2\right)\varepsilon + 2\eta\dot{\varepsilon} = \omega_0^2 - \frac{P}{m_1 l_0} \tag{24}$$

3.2. Free longitudinal oscillations of the tether

For $P = 0$ we get

$$\varepsilon_s = \frac{\omega_0^2}{\left(k^2 + 3\omega_0^2\right)} \tag{25}$$

The dynamic deformation could significantly exceed ε_s, and will depend on the initial conditions of motion of the RSTS. If at the moment of formation of the rotating STS, the projection of the difference between the speeds of the tug $\vec{V}_1$ and the target $\vec{V}_2$ on the direction of the tether is equal to zero (Fig. 2)

$$\left(\vec{V}_2 - \vec{V}_1\right) \cdot \vec{C_1C} = 0 \tag{26}$$

the initial conditions are

$$\varepsilon\,(0) = 0, \quad \dot{\varepsilon}\,(0) = 0. \tag{27}$$

In this case, the stretching of the tether will occur only under the action of the centrifugal force (in a rotating coordinate system). If the velocity of the debris or tug are not perpendicular to the tether at the time of the formation of the tethered system, then the initial conditions will be as follows

$$\varepsilon\,(0) = \varepsilon_0 = 0, \qquad \dot{\varepsilon}\,(0) = \dot{\varepsilon}_0 = \frac{\Delta V_r}{l_0} \tag{28}$$

where

$$\Delta V_r = \left(\vec{V}_2 - \vec{V}_1\right) \cdot \frac{\vec{C_1C}}{\left|\vec{C_1C}\right|}. \tag{29}$$

To obtain the maximum deformation of the tether after the formation of the rotating tethered system, we integrate Eq. (24), provided that the ST thrust does not act on the system ($P = 0$) and the damping coefficient η is zero. We introduce a new variable $v = \dot{\varepsilon}$, and get

$$\ddot{\varepsilon} = \frac{d\dot{\varepsilon}}{dt} = \frac{dv}{d\varepsilon}\frac{d\varepsilon}{dt} = \frac{dv}{d\varepsilon}\ v \tag{30}$$

Now, let us rewrite Eq. (24)

$$\frac{dv}{d\varepsilon}\ v = \omega_0^2 - \varepsilon\left(k^2 + 3\omega_0^2\right). \tag{31}$$

and integrate it

$$\int_{\dot{\varepsilon}_0}^{0} v dv = \int_0^{\varepsilon_{max}} \left[\omega_0^2 - \varepsilon\left(k^2 + 3\omega_0^2\right)\right] d\varepsilon \tag{32}$$

The limits of integration are determined by the fact that at the moment of the maximum deformation of the tether (ε_{max}) caused by the rotation of the system and the possible initial deformation rate $\dot{\varepsilon}_0$ of the tether, the deformation rate will be equal to zero. As a result of integration, we get

$$\frac{1}{2}v^2\Big|_{\dot{\varepsilon}_0}^{0} = \left[\omega_0^2\varepsilon - \frac{1}{2}\varepsilon^2\left(k^2 + 3\omega_0^2\right)\right]\Big|_0^{\varepsilon_{max}} \tag{33}$$

Considering $v_0 = \dot{\varepsilon}_0$, we get

$$-\frac{1}{2}\dot{\varepsilon}_0^2 = \omega_0^2\varepsilon_{max} - \frac{1}{2}\varepsilon_{max}^2\left(k^2 + 3\omega_0^2\right) \tag{34}$$

As a result, we obtain a quadratic equation for the maximum deformation of the tether ε_{max}

$$\left(k^2 + 3\omega_0^2\right)\varepsilon_{max}^2 - 2\omega_0^2\varepsilon_{max} - \dot{\varepsilon}_0^2 = 0 \tag{35}$$

from which the dependence of the maximum deformation of the tether by the initial conditions can be obtained

$$\varepsilon_{max} = \frac{2\omega_0^2 + \sqrt{4\omega_0^4 + 4\left(k^2 + 3\omega_0^2\right)}}{2\left(k^2 + 3\omega_0^2\right)} \tag{36}$$

Next, we transform this expression considering the previously defined expression for the stationary deformation of the tether (25)

$$\varepsilon_{max} = \varepsilon_s\left[1 + \sqrt{1 + \frac{\dot{\varepsilon}_0^2}{\varepsilon_s\omega_0^2}}\right]. \tag{37}$$

From the obtained expression it follows that at zero initial strain rate of the tether ($\Delta V_r = 0$ or $\dot{\varepsilon}_0 = 0$), the maximum deformation of the tether is twice its stationary deformation

$$\varepsilon_{max} = 2\varepsilon_s \tag{38}$$

For $\Delta V_r > 0$ ($\dot{\varepsilon}_0 > 0$) the maximum deformation of the tether will be more than twice the stationary deformation.

The solution to Eq. (24) for $P = 0$ and in the absence of damping is

$$\varepsilon = \varepsilon_s\left(1 - \cos\frac{\omega_0}{\sqrt{\varepsilon_s}}\ t\right) + \frac{\dot{\varepsilon}_0}{\omega_0}\sqrt{\varepsilon_s}\ \sin\frac{\omega_0}{\sqrt{\varepsilon_s}}\ t \tag{39}$$

3.3. Damped energy

In the presence of damping of longitudinal vibrations of the tether, the amplitude of vibrations will decrease ($\dot{l} \to 0$), and the total mechanical energy of the entire system will also decrease. The difference between the initial and final total mechanical energy will make it possible to estimate the energy consumption for damping the tether oscillations after the rotating tethered system formation. At the moment of the formation of the tether connection, the kinetic energy of the system has a maximum and equals to

$$T_0 = \frac{1}{2}\left[m_1 v_1^2 + m_2 v_2^2\right], \tag{40}$$

and the potential energy (Π) is equal to zero since the tether is not yet stretched. In further motion, the tether begins to stretch, increasing its potential energy while the angular velocity of the tethered system decreases.

According to the König's theorem, the kinetic energy of a mechanical system can be represented as the sum of the kinetic energy of motion of the center of mass (T_c) and the energy of motion relative to the center of mass (T_r)

$$T = T_C + T_r \tag{41}$$

The kinetic energy of the system when moving relative to the center of mass is determined by the energy of its rotation around the center of mass and the energy of the longitudinal oscillations of the tether

$$\begin{aligned} 2T_r &= \left[m_1\left(\omega l_1\right)^2 + m_2\left(\omega l_2\right)^2\right] + \left[m_1\dot{l}_1^2 + m_2\dot{l}_2^2\right] = K_r\omega + \dot{l}^2 m_{12} \\ &= \frac{K_r^2}{m_{12}\cdot l^2} + \dot{l}^2 m_{12} \end{aligned} \tag{42}$$

The first term in (42) is the doubled kinetic energy of rotation of the tether system around the center of mass. The second term is the doubled kinetic energy of elastic oscillations of the tether system. In the process of damping the oscillations of the tether, the second term will tend to

zero. The first term will be nonzero since the angular momentum of the K_r system does not change, and the tether length is limited. The kinetic energy of motion of the system relative to the center of mass will tend to the value

$$\lim_{t\to\infty} T_r = T_{rs} = \frac{1}{2}\frac{K_r^2}{m_{12} l_s^2} \tag{43}$$

The stationary value of the tether length l_s is determined by the expression

$$l_s \approx \left[1+\varepsilon_s\right] l_0 = \left[1 + \frac{\omega_0^2}{\left(k^2+3\omega_0^2\right)}\right] l_0 \tag{44}$$

Taking into account (44) the stationary value of the kinetic energy of the rotational motion of the tethered system takes the form

$$T_{rs} = \frac{K_r^2}{2\, m_{12}\cdot\left[1+\varepsilon_s\right]^2\, l_0^2} \tag{45}$$

The value of the kinetic energy of motion of the system relative to the center of mass T_s is completely determined by the initial conditions of motion — the initial angular velocity and the initial length of the tether. The results obtained make it possible to evaluate the work that must be done by the damping devices to damp the longitudinal vibrations of the tether. This value will be determined by the difference between the system's initial and final (stationary) total energy. The initial energy is

$$E_0 = T_c + T_{r0} + \Pi_0 = T_c + \frac{m_{12} l_0^2}{2}\omega_0^2 + \frac{m_{12}}{2} i_0^2 \tag{46}$$

The final energy is

$$E_s = T_c + T_{rs} + \Pi_s = T_c + \frac{K_\omega^2}{2\, m_{12}\left[1+\varepsilon_s\right]^2 l_0^2} + \frac{1}{2}k^2 m_{12}\varepsilon_s^2 l_0^2 \tag{47}$$

The "damped" energy is

$$\begin{aligned} E_d &= T_{rs} + \Pi_s - T_{r0} = \frac{m_{12} l_0^2 \omega_0^2}{2\,\left[1+\varepsilon_s\right]^2} + \frac{1}{2}k^2 m_{12}\varepsilon_s^2 l_0^2 - \frac{m_{12} l_0^2}{2}\omega_0^2 - \frac{m_{12}}{2} i_0^2 \\ &= \frac{1}{2} m_{12} l_0^2 \omega_0^2 \left[\frac{1}{\left(1+\varepsilon_s\right)^2} + \frac{k^2}{\omega_0^2}\varepsilon_s^2 - \frac{i_0^2}{l_0^2\omega_0^2} - 1\right]. \end{aligned} \tag{48}$$

For $\varepsilon_s \ll 1$ we get

$$E_d \approx -2\, T_{r0}\varepsilon_s - \frac{m_{12}}{2} i_0^2 \tag{49}$$

The results obtained make it possible to estimate the energy level required for active damping of longitudinal vibrations of the cable. The propulsion system of the ST [14] or a tether length control system [16] can be used for active damping.

The results show that unwanted longitudinal vibrations in the tether depend on the initial conditions of the tug–debris relative motion. To reduce the tether tension, it is necessary at the time of the system's formation to ensure the fulfillment of the condition $\dot{\varepsilon}_0 = 0$. In this case, the maximum deformation of the tether will only be twice the stationary deformation. For $\dot{\varepsilon}_0 > 0$ this value can be several times larger. Let us consider how the relative orbital motion of the tug and the space debris object affects the longitudinal vibrations of the tether.

4. Interception orbit

4.1. Relative motion of the space tug

Let us consider motion of the space tug relative to the debris object orbiting circular orbit in a debris local vertical local horizontal rotating frame, called the Euler–Hill frame, as shown in Fig. 7. The figure shows space debris object with Euler–Hill frame $C_2 x_o y_o z_o$, space tug and ADM.

Position of the space tug and ADM relative to the debris is defined by the vectors ρ_1 and ρ_a respectively in Euler–Hill frame. The motion of the space tug relative to the debris object in the orbital plane of the SD orbiting circular orbit can be described by the equations [17]

$$x_1 = 4x_{10} + \frac{2\dot{y}_{10}}{n_2} + \frac{\dot{x}_{10}}{n_2}\sin n_2 t - \left(3x_{10} + \frac{2\dot{y}_{10}}{n}\right)\cos n_2 t \tag{50}$$

$$y_1 = \left(y_{10} - \frac{2\dot{x}_{10}}{n_2}\right) - \left(6n_2 x_{10} + 3\dot{y}_{10}\right) t + \left(6x_0 + \frac{4\dot{y}_{10}}{n_2}\right)\sin n_2 t + \frac{2\dot{x}_{10}}{n_2}\cos n_2 t \tag{51}$$

$$z_1 = \frac{\dot{z}_{10}}{n_2}\sin n_2 t + z_{10}\cos n_2 t \tag{52}$$

where $\rho_{10} = \left(x_{10}, y_{10}, z_{10}\right)^T$, $\dot{\rho}_{10} = \left(\dot{x}_{10}, \dot{y}_{10}, \dot{z}_{10}\right)^T$ are the position and velocity of the ST relative to the debris for $t = 0$; $n_2 = \sqrt{\mu r_2^{-3}} = \text{const}$ is the mean motion of the SD. Further we suppose that the ST is orbiting in the same orbital plane as space debris object $z_{30} = 0$, $\dot{z}_{10} = 0$.

Fig. 8 shows the interception trajectory of the ST relative to the SD and the position of the ST relative to the SD when the tether starts to strain. If the tether starts straining at $t = t_0$ the $\Delta\mathbf{V}_r$ projection is equal to zero. If the tether starts straining at $t_0 + \Delta t$ the difference velocity vector has projection of the tether line ($\Delta\mathbf{V}_r > 0$). The position of the space tug on Fig. 8 is not ideal in terms of minimization of $\Delta\mathbf{V}_r$ projection.

The interception orbit should be constructed such that the difference in orbital velocities of debris and space tug is perpendicular to the tether at t_0. Let us parametrize the initial position and velocity of the space tug at t_0 as

$$\rho_1 = \begin{bmatrix} x_{10} \\ y_{10} \\ z_{10} \end{bmatrix} = l_0 \begin{bmatrix} \cos\varphi_0 \\ \sin\varphi_0 \\ 0 \end{bmatrix} \tag{53}$$

$$\dot{\rho}_1 = \begin{bmatrix} \dot{x}_{10} \\ \dot{y}_{10} \\ \dot{z}_{10} \end{bmatrix} = \Delta V_0 \begin{bmatrix} \sin\varphi_0 \\ -\cos\varphi_0 \\ 0 \end{bmatrix} - \mathbf{n}_2 \times \boldsymbol{\rho}_1 \tag{54}$$

where $\mathbf{n}_2 = \left[0, 0, n_2\right]^T$ is the angular velocity of the $Ox_o y_o z_o$ frame, ΔV_0 is the desired difference in the orbital velocities of the space tug and debris object, l_0 is the desired distance between the tug and the debris object (equals to the initial free length of the tether) at t_0. The second term in (54) takes into account rotation of the Hill-frame with the angular rate n_2. The position of the ST relative to the SD is determined by the length of the tether l_0 and the angle φ_0 between the tether line and the Ox_0 axis. By setting the values of l_0, φ_0, and ΔV_0, different interception orbits can be determined. Freezing the rotating frame $C_2 x_o y_o z_o$, one can obtain the position and velocity vectors of the space tug relative to the Earth

$$\mathbf{r}_1 = r_2 \begin{bmatrix} 1 \\ 0 \\ 0 \end{bmatrix} + \boldsymbol{\rho}_1, \quad \mathbf{V}_1 = \mathbf{V}_2 + \Delta V_0 \begin{bmatrix} \sin\varphi_0 \\ -\cos\varphi_0 \\ 0 \end{bmatrix} \tag{55}$$

and get the parameters of the interception orbit. We can write down the energy integral [18] of the unit mass (J/kg)

$$H_1 = V_1^2 - 2\frac{\mu}{r_1} \tag{56}$$

angular momentum integral

$$\mathbf{c}_1 = \mathbf{r}_1 \times \mathbf{V}_1 \tag{57}$$

and obtain basic parameters of the intercept orbit

$$p_1 = \frac{c_1^2}{\mu}, \quad e_1 = \sqrt{1 + \frac{c_1^2}{\mu^2} H_1}, \quad a_1 = -\frac{\mu}{H_1} \tag{58}$$

where p_1 is the latus rectum, e_1 is the eccentricity, a_1 is the semimajor axis.

Table 1 shows the perigee and apogee heights and energy integral of the interception orbits for different values of angle φ_0. The lowest energy integral has the orbit constructed with $\varphi_0 = 180$ degrees. That

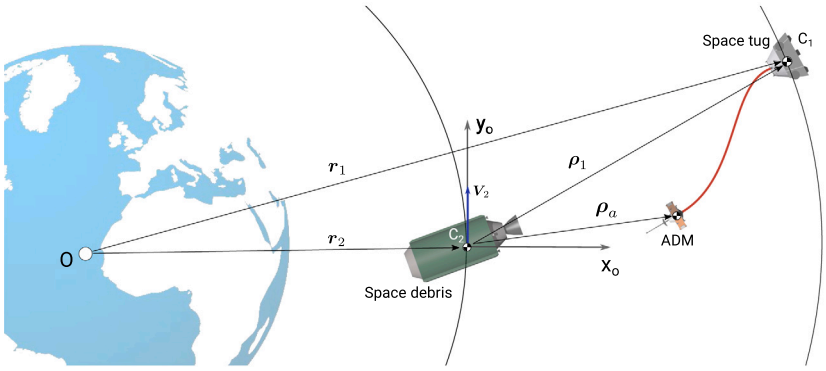

Fig. 7. Motion of the space tug relative to the space debris.

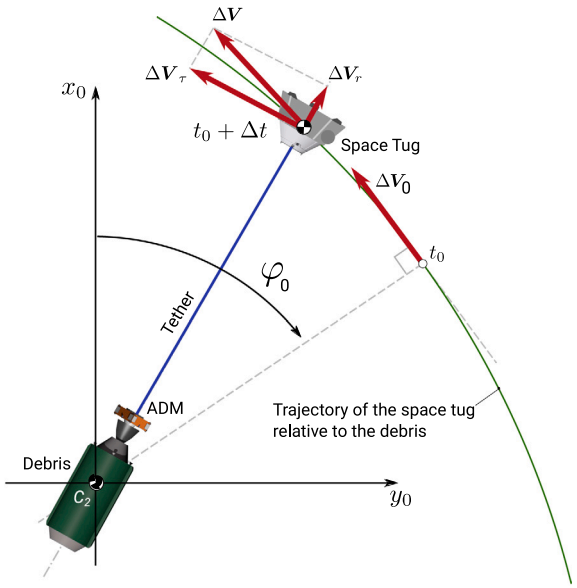

Fig. 8. The relative position of the ST and SD.

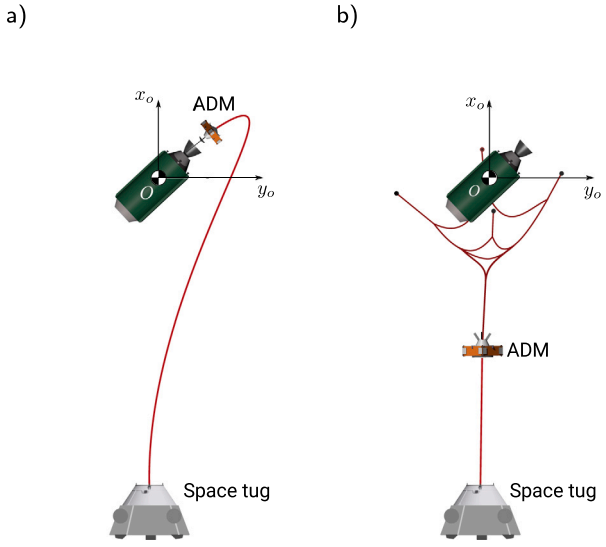

Fig. 9. Gripping the space debris object by a probe-cone device and by a tethered net.

Table 1
Perigee and apogee heights of interception orbit for l_0 = 1 km, $|\Delta V|$ = 50 m/s and circular orbit of the SD object h_2 = 800 km.

φ_0, deg	ΔV_0, m/s	h_{1p}, km	h_{1a}, km	H_1, MJ/kg
0	50	613.7	801.0	−56.313
45	50	659.5	809.2	−56.099
90	50	751.2	849.4	−55.583
135	−50	656.1	807.0	−56.121
180	−50	607.9	799.0	−56.344

orbit is an inner orbit relative to the orbit of the SD and has apogee height lower than the orbit SD height by l_0. This orbit is the best-cost interception orbit if the ST is injected into that orbit from the Earth's surface.

On the other hand, angle φ_0 could be constrained by the angular position of the space debris object at t_0. Some gripping devices could pose an additional operational constraint for the interception trajectory design. For example, a probe-cone device utilizes the nozzle of the space debris object as a docking port, so at t_0, the space debris object must be oriented with its nozzle towards the space tug. It will prevent the tether from becoming tangled (Fig. 9a). Another gripping device does not pose additional constraints for the φ_0 angle. For example, a tethered net could capture the debris object from any side (Fig. 9b).

4.2. Interception algorithm

The results obtained make it possible to formulate an algorithm for intercepting a space debris object using ADM. At the first phase, we should calculate ω_0 for the given value of the tug's thrust

$$\omega_0 = k_\omega \sqrt{\frac{P}{m_1 l_0}} \tag{59}$$

where $k_\omega \approx 1.3 \ldots 1.5$ is the safety factor. At the second phase, for the obtained ω_0 and given value of the tether length l_0 we get the required ΔV_0

$$\Delta V_0 = \omega_0 l_0 + n_2 l_0 \tag{60}$$

As noted above, the value of φ_0 angle depends on the gripping device type installed on the ADM and the orientation of the space tug. At the third phase, the trajectory of the space tug relative to the debris object is obtained using the expression (50)–(52) in backward time from t_0 to $t_{ADM} = t_0 - \Delta t_{ADM}$, where t_{ADM} is the time of ADM separation from the space tug.

The time interval Δt_{ADM} is determined by the capabilities of the ADM propulsion system (thrust-to-weight ratio of the ADM) and the capabilities of the ADM control system. The ADM control system should lock on the SD before the separation from the ST, so the distance between the ADM and the SD should be in the range of the ADM sensors. On the other hand, this distance should not be too small for the ADM propulsion system to approach and capture the SD within the

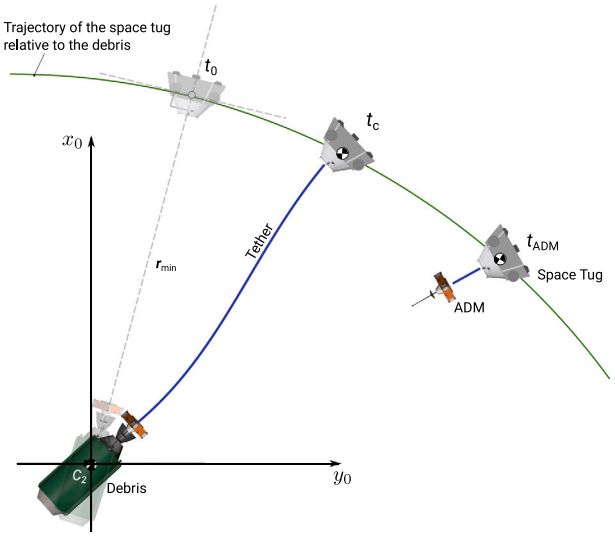

Fig. 10. Interception trajectory.

time-interval Δt_{ADM}. The impulses for intercepting the debris can be estimated as follows. The first impulse is [17]

$$\Delta \mathbf{u}_{a1} = -\frac{n_2}{a}\begin{bmatrix} -4x_{10}s + 3x_{10}n_2\ \Delta t_{ADM}c + 2y_{10} - 2y_{10}c \\ -14x_{10}s + 14x_{10}c + 6n_2x_{10}\Delta t_{ADM}s - y_{10}s \\ z_{10}n_2\cot(\Delta t_{ADM}n) \end{bmatrix} - \dot{\rho}_1\left(t_{ADM}\right) \quad (61)$$

where

$$a = 8c - 8 + 3n_2\Delta t_{ADM}s, \quad c = \cos(n_2\Delta t_{ADM}), \quad s = \sin(n_2\Delta t_{ADM}) \quad (62)$$

$\mathbf{V}_1\left(t_{ADM}\right)$ is the velocity of the space tug during the separation of the ADM. After the first impulse the ADM has the following velocity relative to the debris

$$\dot{\rho}_a^+ = \dot{\rho}_1\left(t_{ADM}\right) + \Delta \mathbf{u}_{a1} = \begin{bmatrix} \dot{x}_a^+ \\ \dot{y}_a^+ \\ \dot{z}_a^+ \end{bmatrix} \quad (63)$$

The second impulse is

$$\Delta \mathbf{u}_{a2} = -\begin{bmatrix} \dot{x}_a^+ c + (3x_{10}n_2 + 2\dot{y}_a^+)s \\ \left(6x_{10}n_2 + 4\dot{y}_a^+\right)c - \left(6n_2x_{10} + 3\dot{y}_a^+\right) - 2\dot{x}_a^+ s \\ \dot{z}_a^+ c - z_{10}n_2 s \end{bmatrix} \quad (64)$$

During the time-interval $[t_{ADM},\ t_0]$, the tether control system installed on the space tug uncoil the tether while the ADM approaches the debris object. At t_0, the tether length is fixed, the tether starts straining, and the STS starts rotating (see Fig. 10).

The ST achieves the interception orbit with some errors so that the actual interception trajectory could deviate from the nominal interception trajectory defined by (55) Fig. 11 shows the nominal interception trajectory and the actual interception trajectory of the ST. The figure also shows the range of the distance $[l_{min}, l_{max}]$ determined by the amount of the tether on-board the ST.

5. Example

In this section, a numerical example is handled to illustrate the construction procedure of the interception orbit and the effect of the moment of formation of the RSTS on the tether deformation. To do this, we consider a nominal interception orbit and the actual interception orbit that slightly differs from the nominal orbit. In this section, the result of the simplified model is also compared with the numerical simulation of the more complex model of the orbital motion of the RSTS.

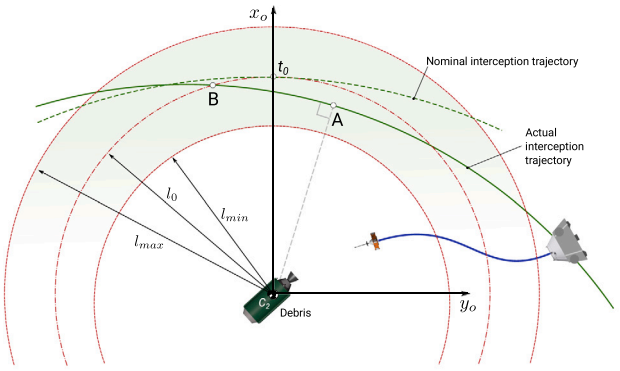

Fig. 11. Nominal and actual interception orbits.

Table 2
Parameters of the system and initial conditions.

Parameter	Value
Mass of the space tug, m_1, kg	1200
Mass of the debris, m_2, kg	1500
Nominal initial tether length, l_0, m	2000
Position of the ST relative to SD, φ_0, deg	0
Initial relative velocity, ΔV_0, m/s	50
Young's modulus of the tether, E, GPa	124
Tether strength σ, GPa	3.34
Critical unit deformation, $\varepsilon_\sigma(k_\sigma = 1)$, %	2.69
Tether diameter, d, mm	2

5.1. Parameters of the system and initial conditions

The interception of a SD object with a mass of 1500 kg orbiting in a circular orbit with a height of 800 km is considered. The ST has a mass of 1200 kg. The parameters of the considered system are presented in Table 2. The tether is made of Spectra-2000. For ΔV_0 = 50 m/s, l_0 = 2 km and $\varphi_0 = 0$ we can calculate the parameters of the nominal interception orbit of the space tug using the expression (50)–(58): perigee height h_{1p} = 616.6 km, and apogee h_{1a} = 802.0 km. The RSTS starts rotating at $t = t_0$ when the space tug is higher than the debris object. Let us suppose that the ADM separates from the ST at Δt_{ADM} = 120 s before t_0.

5.2. Simulation results

ADM separates from the ST at $t_{ADM} = t_0 - 120$ s. At time interval $[t_{ADM}, t_0]$ ADM approaches the SD object and captures it. At this time interval, the tether control system of the ST increases the free length of the tether. At $t = t_0$ the tether control system fixes the tether's length to l_0 = 2000 m. The initial angular velocity of the RSTS is ω_0 = 2.87 deg/s. The maximum unit deformation of the tether ε_{max} = 1.67 % is twice of the stationary deformation ε_s = 0.83 %. The maximum deformation does not exceed the critical deformation ε_σ. Fig. 12 shows nominal interception trajectory which starts at point S_1. If the ST follows the nominal trajectory the STS starts to rotate when the coordinates of the ST relative to the SD reach x_o = 2 km, $y_o = 0$ in the Euler–Hill frame of the SD $C_2x_oy_oz_o$ (Fig. 12).

Next, let us compare the nominal interception trajectory with the actual trajectory. The nominal interception trajectory is tangent to the circle with a radius of l_0. Let us suppose that at t_{ADM} time the space tug is displaced from the nominal position by Δx_o = 1950 m along x_o axis and by Δy_o = 671 m along y_o axis (Fig. 12). The actual orbit of the space tug in this case is h_{1p} = 455.5 km, h_{1a} = 802.6 km. Fig. 12 shows the nominal and actual trajectories of the ST relative to the SD. The nominal interception trajectory is tangent to the circle with a radius of l_0, but the actual trajectory crosses that circle. The RSTS can be formed

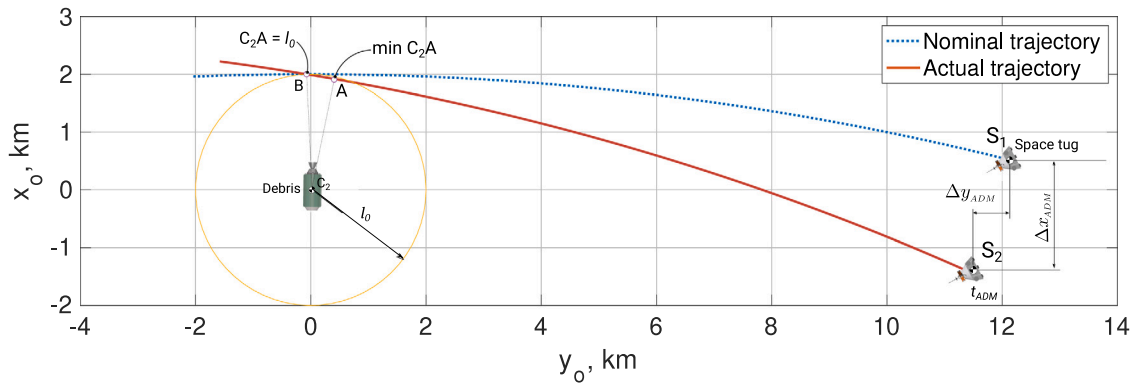

Fig. 12. Nominal and actual trajectories of the ST and ADM relative to the SD.

a) Distance between the ST and SD

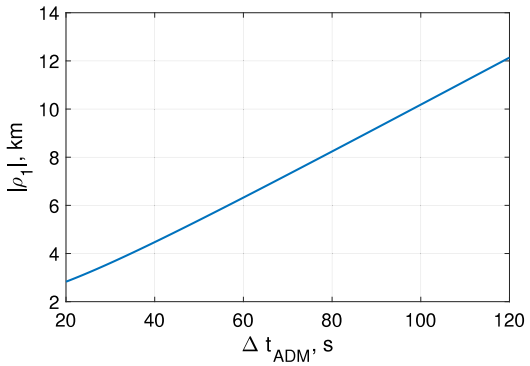

b) Total velocity change of the ADM

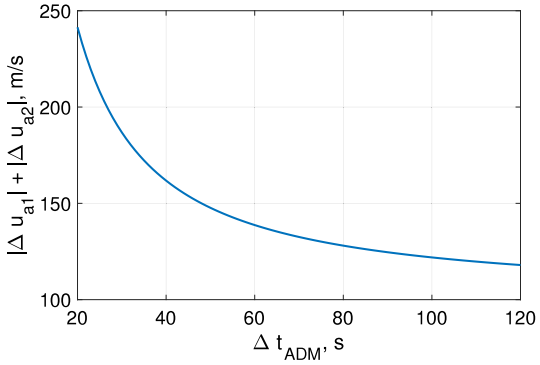

Fig. 13. Distance between the ST and SD at $t = t_{ADM}$ and total delta-V of the ADM.

Table 3
Nominal and actual interception trajectory.

Parameter	Nominal	Actual (A)	Actual (B)
$h_{1p} \times h_{1a}$, km	433 × 802	455.5 × 802.6	455.5 × 802.6
$\lvert\Delta \boldsymbol{u}_{a1}\rvert + \lvert\Delta \boldsymbol{u}_{a2}\rvert$, m/s	118	113	113
d, m	2000	1960	2000
ΔV_r, m/s	0.0	0.0	18.9
ΔV_n, m/s	100.0	97.0	95.2
ω_0, deg/s	2.9	2.8	2.7
ε_s, %	0.83	0.82	0.76
ε_{max}, %	1.67	1.64	2.65

at point A, where the distance between the ST and SD has a minimum, or at point B, where the distance is equal to l_0.

Table 3 shows parameters of nominal and actual trajectories of the ST and parameters of the rotating STS for two cases. The Actual (A) case corresponds to the forming of the STS when the distance between the ST and SD is minimal (point A on Fig. 12). The actual (B) case corresponds to the forming of the STS when the distance between the ST and SD is equal to l_0 (point B on Fig. 12).

Total delta-V of the ADM ($|\Delta \mathbf{u}_{a1}| + |\Delta \mathbf{u}_{a2}|$) depends on the initial distance between the space tug and debris object and that distance depends on the Δt_{ADM}. Fig. 13a shows the distance between the space tug and debris $|\rho_1|$ as function of Δt_{ADM}. $|\rho_1|$ is obtained from the expressions (53)–(55) for $t = -\Delta t_{ADM}$. Fig. 13b shows the dependence of the total delta-V from the Δt_{ADM}. The total delta-V of the ADM is not less than ΔV and increases with decreasing the Δt_{ADM}.

The results show that forming of the rotating STS at point B leads to a noticeable increase of the maximal deformation of the tether (from 1.67% to 2.65%). The unit deformation does not exceed critical deformation $\varepsilon_\sigma = 2.7\%$. The results show that the rotating STS should be formed when the distance between the space tag and debris is minimal (A), so the tether control system should fix the tether length when it starts to increase.

The tether length could be fixed later with the delay Δt due to errors of the tether control system. In this case, the relative velocity of the ST becomes non-perpendicular to the tether line, and ΔV_r projection is increasing. ΔV_τ is decreasing, so the initial angular rate of the STS is decreasing. The maximum deformation of the tether increases with increasing ΔV_r projection. Fig. 14 shows the stationary unit deformation of the tether ε_s and maximum unit deformation of the tether ε_{max} as functions of Δt is Fig. 14 also show critical unit deformation of Spectra-2000 tether with diameter of 2 mm $\varepsilon_\sigma = 2.7\%$. For Δt greater than 4 s the unit deformation ε_{max} become greater than critical unit deformation ε_σ. The tether with diameter of 2 mm fails with these initial conditions.

5.3. Validation of the model

Let us compare the results obtained by the simplified model (39) with the result of direct numerical integration of the motion of two rigid bodies, connected by a massless elastic tether in gravitational field. The motion of the bodies is considered relative to the inertial frame $EX_EY_EZ_E$ with the origin in the center mass of the Earth (Fig. 15). The motion equations for the center mass of the ST ($i = 1$) and SD ($i = 2$) are

$$m_1 \ddot{\boldsymbol{r}}_1 = m_1 \boldsymbol{a}_{G1} + \boldsymbol{e}_t T + \boldsymbol{A}_1 \boldsymbol{P} \tag{65}$$

$$m_2 \ddot{\boldsymbol{r}}_2 = m_2 \boldsymbol{a}_{G2} - \boldsymbol{e}_t T \tag{66}$$

On the right side of the first equation of the ST motion are the gravitational force of the Earth $m_1 \boldsymbol{a}_{G1}$, tether tension force $\boldsymbol{e}_t T$ and

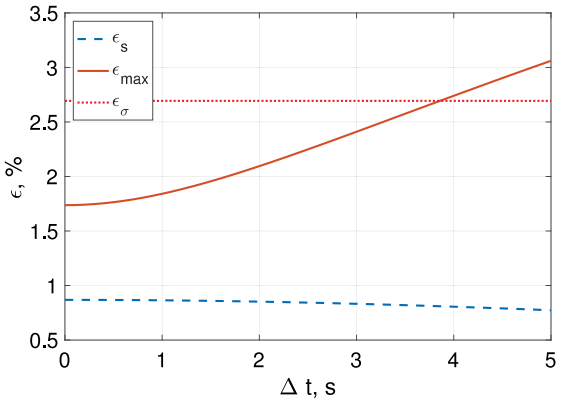

Fig. 14. Stationary (ϵ_s), maximum (ϵ_{max}) unit deformations of the tether as functions of Δt and ultimate tensile strain (ϵ_σ).

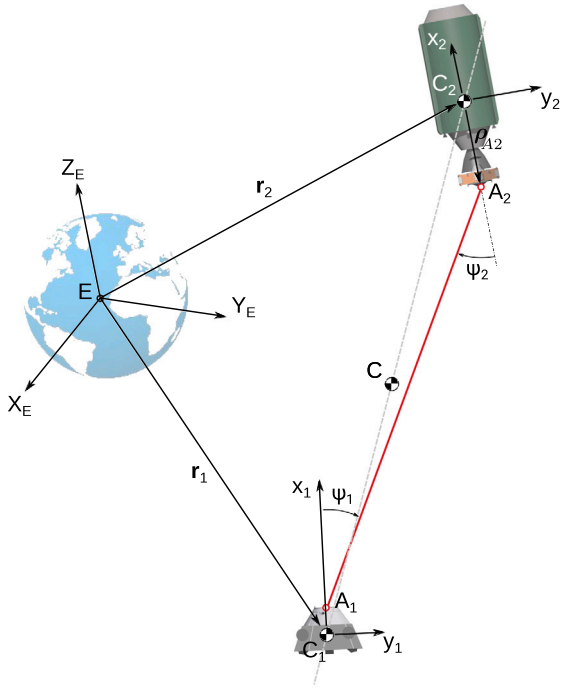

Fig. 15. Two rigid bodies connected by the tether.

the tug's thrust force $\boldsymbol{P}$. On the right side of the SD motion equation are the gravitational force of the Earth and the tether tension force. $\boldsymbol{r}_1 = (x_1, y_1, x_1)^T$ is the column vector of the ST position relative to the Earth's center, $\boldsymbol{r}_2 = (x_2, y_2, x_2)^T$ is the position column vector of the SD relative to the Earth's center, $\boldsymbol{e}_t$ is the unit vector of the tether line

$$\boldsymbol{e}_t = \frac{\boldsymbol{r}_{A2} - \boldsymbol{r}_{A1}}{|\boldsymbol{r}_{A2} - \boldsymbol{r}_{A1}|} \tag{67}$$

$\boldsymbol{r}_{Ai}$, $i = 1, 2$ is the tether connection point column vector relative to the $EX_EY_EZ_E$ frame

$$\boldsymbol{r}_{Ai} = \boldsymbol{r}_i + \boldsymbol{A}_i \boldsymbol{\rho}_{Ai}, \quad i = 1, 2 \tag{68}$$

$\boldsymbol{A}_i$ is the transformation matrix from the coordinate system $C_i x_i y_i z_i$ to the system $EX_EY_EZ_E$, $\boldsymbol{\rho}_{Ai}$ is the column vector of the tether attachment point on the body i in body frame $C_i x_i y_i z_i$. $\boldsymbol{a}_{Gi}$ is the gravity acceleration of the Earth with J_2 term [19]

$$\boldsymbol{a}_{Gi} = -\frac{\mu}{r_i^3}\boldsymbol{r}_i + \frac{3}{2}\frac{\mu}{r_i^5} J_2 R_E^2 \begin{bmatrix} x_i\left(5\frac{z_i^2}{r_i^2} - 1\right) \\ y_i\left(5\frac{z_i^2}{r_i^2} - 1\right) \\ z_i\left(-3 + 5\frac{z_i^2}{r_i^2}\right) \end{bmatrix} \tag{69}$$

where $R_E = 6378$ km is the mean equatorial radius of the Earth, μ is the Earth's gravitational parameter, x_i, y_i, and z_i are the magnitude of the components of the position vector of the ST ($i = 1$) and SD ($i = 2$). T is the tether tension force

$$T = \begin{cases} (|\boldsymbol{r}_{A2} - \boldsymbol{r}_{A1}| - l_0)c, & d \geq 0 \\ 0, & d < 0 \end{cases} \tag{70}$$

where

$$d = A_1A_2 = (|\boldsymbol{r}_{A2} - \boldsymbol{r}_{A1}| - l_0) \tag{71}$$

$\boldsymbol{P} = [P, 0, 0]^T$ is the tug's thrust. We suppose that the tug's thrust is applied along the longitudinal axis of the space tug and does not induces torques relative to the center mass of the space tug. The attitude motions of the bodies are described by the following equations

$$\boldsymbol{J}_1\dot{\boldsymbol{\omega}}_1 = -\boldsymbol{\omega}_1 \times \boldsymbol{J}_1\boldsymbol{\omega}_1 + \boldsymbol{\rho}_{A1} \times \boldsymbol{e}_t \boldsymbol{A}_1^T T \tag{72}$$

$$\boldsymbol{J}_2\dot{\boldsymbol{\omega}}_2 = -\boldsymbol{\omega}_2 \times \boldsymbol{J}_2\boldsymbol{\omega}_2 - \boldsymbol{\rho}_{A2} \times \boldsymbol{e}_t \boldsymbol{A}_2^T T \tag{73}$$

$\boldsymbol{J}_1$, $\boldsymbol{J}_2$ are the inertia tensors of the ST and SD objects. These equation should be supplemented with the kinematic equations for the cosine matrices of the space tug and debris

$$\dot{\boldsymbol{A}}_i = \boldsymbol{A}_i\tilde{\boldsymbol{\omega}}_i \tag{74}$$

where $\tilde{\boldsymbol{\omega}}_i$ is the skew symmetric matrix of angular velocity components

$$\tilde{\boldsymbol{\omega}}_i = \begin{bmatrix} 0 & -\omega_{iz} & \omega_{iy} \\ \omega_{iz} & 0 & -\omega_{ix} \\ -\omega_{iy} & \omega_{ix} & 0 \end{bmatrix} \tag{75}$$

The Eqs. (65) and (66) are integrated with the initial conditions that are equivalent to the initial conditions for the point B of the actual interception orbit. The parameters of the tether are presented in Table 2. The inertia tensor of the ST is $\boldsymbol{J}_1 = \text{diag}(1000, 2000, 2000)$, and the inertia tensor of the SD is $\boldsymbol{J}_2 = \text{diag}(1000, 5000, 5000)$. The SD object orbits in a circular orbit with the height $h_{2p} = h_{2a} = 800$ km and inclination of $i_2 = 98°$. The ST orbit in an elliptic orbit $h_{1p} = 455.5$ km, $h_{1a} = 802.6$ km in the same orbital plane. The tether attachment point in the ST frame $C_1x_1y_1z_1$ is defined by the columns vector $\boldsymbol{\rho}_{A1} = [3, 0, 0]^T$ m. The thrust of the ST is 4.5 kN. The tether attachment point in the SD frame $C_2x_2y_2z_2$ is defined by the columns vector $\boldsymbol{\rho}_{A2} = [-3, 0, 0]^T$ m. The STS starts to rotate when the SD object crosses the Earth's equatorial plane. The longitudinal axes of the SD (C_2x_2) and ST (C_1x_1) are aligned with the tether line and C_1y_1, C_2y_2 axes are perpendicular to the orbital plane of the center mass of the system, so the initial conditions of the motion are

$$\boldsymbol{r}_2(0) = [7171003, 0, 0]^T \text{ m}, \ \boldsymbol{v}_2 = [0, -1115, 7372]^T \text{ m/s}, \tag{76}$$

The column vector of the initial position of the space tug is

$$\boldsymbol{r}_1(0) = \boldsymbol{r}_2(0) + \boldsymbol{A}_{EO}\boldsymbol{\rho}_{21}(0), \tag{77}$$

where $\boldsymbol{\rho}_{21}(0)$ the position of the ST relative to SD when the STS begins to rotate

$$\boldsymbol{\rho}_{21}(0) = [1.998, -0.0681, 0]^T \text{ km}. \tag{78}$$

$\boldsymbol{A}_{EO}$ is the transformation matrix from the Euler–Hill frame of the SD to the $EX_EY_EZ_E$ frame composed by the unit vectors of the Euler–Hill frame

$$\boldsymbol{A}_{EO} = \begin{bmatrix} \boldsymbol{e}_r & \boldsymbol{e}_t & \boldsymbol{e}_n \end{bmatrix}$$

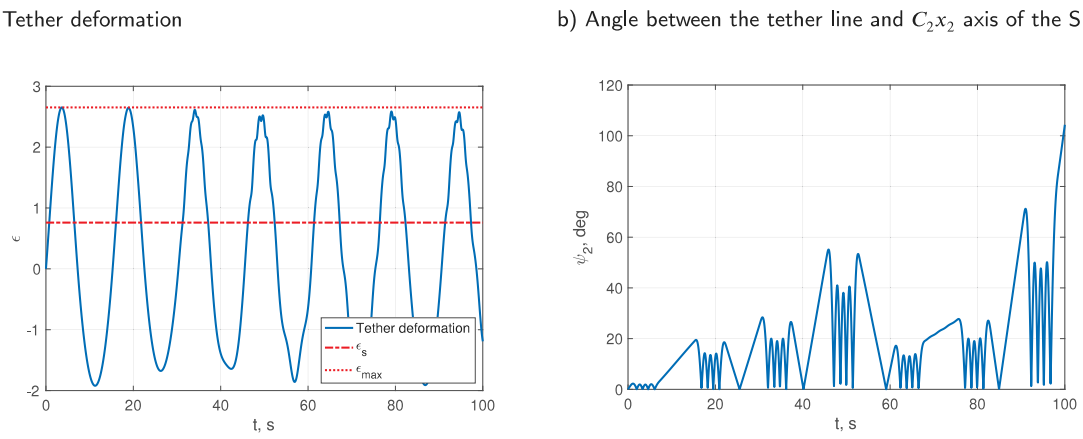

Fig. 16. Tether deformation and the angle between the tether line and the longitudinal axis of the SD.

$\boldsymbol{e}_r = \boldsymbol{r}_1(0)/|\boldsymbol{r}_1(0)|$, $\boldsymbol{e}_n = (\boldsymbol{r}_1(0)\times\boldsymbol{V}_1(0))/|\boldsymbol{r}_1(0)\times\boldsymbol{V}_1(0)|$, $\boldsymbol{e}_n = \boldsymbol{r}_1(0)\times\boldsymbol{V}_1(0)$, $\boldsymbol{e}_t = \boldsymbol{e}_n \times \boldsymbol{e}_r$ Orientation matrices of the bodies for $t = 0$ are

$$\boldsymbol{A}_i = [\boldsymbol{e}_{12}, \boldsymbol{e}_n \times \boldsymbol{e}_{12}, \boldsymbol{e}_{12}] \tag{79}$$

where $\mathbf{e}_{12}$ is the unit vector aligned with the line that connecting the center of masses of the ST and SD

$$\boldsymbol{e}_{12} = \frac{\boldsymbol{r}_2 - \boldsymbol{r}_1}{|\boldsymbol{r}_2 - \boldsymbol{r}_1|} \tag{80}$$

We suppose that all components of angular velocities of the ST and SD in $EX_EY_EZ_E$ frame are equal to zero.

Fig. 16a shows the deformation of the tether during 100 s time interval after the STS begins to rotate. The figure also shows the static and maximum deformation of the tether obtained using the formulas (25) and (37). We can see that estimation of the maximum deformation agrees with the numerical simulation results.

Fig. 16a is obtained by numerical integration of the Eqs. (65), (66) and (72), (73) without damping of the tether so we can see the time intervals when the deformation of the tether falls below zero. At these intervals the tether is slacked and the stability of the STS is lost. Fig. 16b shows the time history of the angle between the longitudinal axis of the SD and the tether line ψ_2 ($\psi_2 \geq 0$). We can see buildup of the SD oscillation relative to the tether. The ψ_2 angle reaches 100 degrees after 100 s which means that the tether could be tangled. Fig. 16a also shows the influence of the oscillation of the SD relative to the tether on the tether longitudinal oscillations. The oscillations of a higher frequency, caused by the motion of the SD, are superimposed on the tether oscillations with a period of about 20 s.

To avoid large oscillations of the SD the longitudinal oscillations of the tether should be damped. Fig. 17a shows the time history of the tether deformation when the tether oscillation is damped by using tug's thrust. The simple control algorithm is used to illustrate the effect of the active damping to the attitude motion of the SD relative to the tether. The tug's thruster is on when the tether deformation is greater than zero and the deformation velocity is greater than 1 m/s. Fig. 17a also shows the tug's thrust time history. Fig. 17b shows the time history of the angle between the longitudinal axis of the SD and the tether line. The maximum angle does not reach 3 deg/s when the tether oscillations are damped.

Next, let us show the influence of the gravitational perturbations on the RSTS motion. Fig. 18 shows the time history of the angle between the tether and the orbital plane of the RSTS. The J2 term induces the out-of-plane oscillations of the RSTS. The maximum angle does not exceed 0.1 deg after one orbital period of the RSTS. The results in [14] illustrate that the transfer of the SD to the disposal orbit from 800 km circular orbit takes less than one hour if the ST is equipped with the high thrust propulsion system, so the out-of-plane oscillation of the RSTS could be neglected. The impact of the gravity perturbations should be considered for long-term de-orbit missions when the ST is equipped with a low thrust propulsion system.

6. Conclusion

Linearized equations of longitudinal oscillations of RSTS is developed. The developed model makes it possible to estimate the maximum deformation of the tether and select the parameters of the tether (material, diameter) for the expected initial conditions of the relative motion of the ST and SD. The linearized model is validated by comparison with numerical solution.

The algorithm of construction of the interception orbit for the ST is proposed. The interception orbit is parametrized by the three parameters (ΔV_0, l_0, φ_0) that define desired initial conditions of the RSTS. The first two parameters affect the initial angular rate of the RSTS, and the last one defines the position of the space tug relative to the debris at the moment of forming RSTS and could depend on the constraints imposed by the gripping device and the attitude motion of the space tug. If the ADM is equipped with a tethered net gripping device, then φ_0 could be selected from the viewpoint of minimization of the interception orbit energy.

The obtained results show a significant effect of the projection of the relative velocity on the direction of the tether on the maximum deformation. This effect should be taken into account when constructing the interception orbit of the ST. For the moment of formation of the RSTS, it is advisable to take the moment of the minimum distance between the ST and SD. That reduces the projection of the relative velocity to the direction of the tether. The tether length control system can be used to determine this point in time. After the separation of the ADM from the ST, the length of the tether increases. In the process of approaching the ADM with the SD, the control system should not interfere with the tether pulling, creating a minimum tether tension in case of maneuvers by the ADM. After gripping the SD by the ADM, the tether control system should track the change in the tether length. An increase in the length of the tether is a signal for its fixation and the formation of the RSTS. Global navigation systems can be used to determine the distance between the tug and the space debris object. Receivers of GNS signals could be installed on the ADM and the ST to measure the relative velocity and distance between them and use this information to determine the moment of fixing the tether length and forming the RSTS.

After the formation of the RSTS, oscillations of the ST and SD relative to the tether will occur. To eliminate the buildup of these oscillations, the longitudinal oscillations of the tether should be damped by using tug's thrust or by controlling the free length of the tether.

Considered RSTS can be used for ADR of large debris objects like spent upper stages of the rockets or unfunctional satellites. ADR using RSTS allows to simplify the adaptation of the existing upper stages of the rockets for towing using pushing scheme task by delegation of all specific ADR tasks (rendezvous, gripping) to the ADM. That allows using proposed RSTS for piggyback ADR mission utilizing residual capability of the upper stages.

a) Tether deformation

b) Angle between the tether line and C_2x_2 axis of the SD

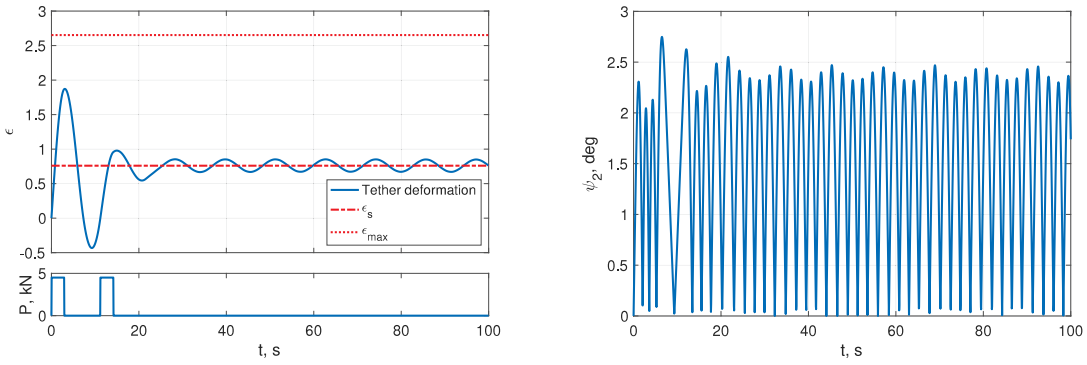

Fig. 17. Tether deformation and the angle between the tether line and the longitudinal axis of the SD (the oscillations of the tether are damped).

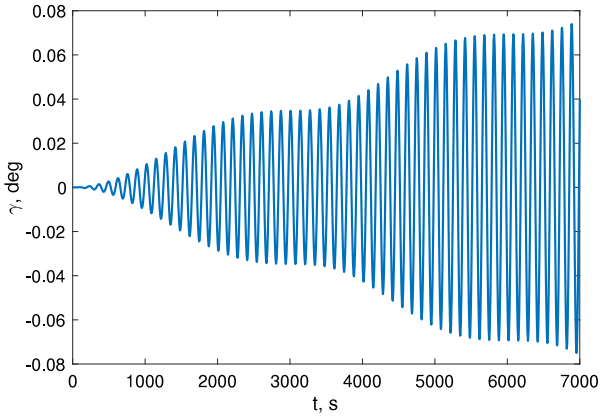

Fig. 18. Angle between the tether and the orbital plane of the RSTS.

Declaration of competing interest

The authors declare that they have no known competing financial interests or personal relationships that could have appeared to influence the work reported in this paper.

Acknowledgment

Research supported by the project of the Omsk State Technical University on internal research project No. 21185B, October 29, 2021.

References

[1] A. Flores-Abad, O. Ma, K. Pham, S. Ulrich, A review of space robotics technologies for on-orbit servicing, Prog. Aerosp. Sci. 68 (2014) 1–26, http://dx.doi.org/10.1016/j.paerosci.2014.03.002.

[2] M. Ansdell, Active space debris removal: Needs, implications, and recommendations for today's geopolitical environment, J. Public Int. Aff. 21 (1) (2010) 16.

[3] M. Shan, J. Guo, E. Gill, Review and comparison of active space debris capturing and removal methods, Prog. Aerosp. Sci. 80 (2015) 18–32, http://dx.doi.org/10.1016/j.paerosci.2015.11.001.

[4] N. Ortiz Gómez, S.J.I. Walker, M. Jankovic, J.M. Romero Martín, F. Kirchner, M. Vasile, Control analysis for a contactless de-tumbling method based on eddy currents: problem definition and approximate proposed solutions, AIAA Guid. Nav. Control Conf. (January) (2016) 1–25.

[5] U. Battista, A. Landini, W. Gołębiowski, R. Michalczyk, Design of net ejector for space debris capturing, in: T. Flohrer, F. Schmitz (Eds.), 7th European Conference on Space Debris, Darmstadt, Germany, April, ESA Space Debris Office, Darmstadt, 2017, pp. 18–21.

[6] H. Hakima, M.R. Emami, Assessment of active methods for removal of LEO debris, Acta Astronaut. 144 (December 2017) (2018) 225–243, http://dx.doi.org/10.1016/j.actaastro.2017.12.036.

[7] L. Jasper, H. Schaub, Input shaped large thrust maneuver with a tethered debris object, Acta Astronaut. 96 (1) (2014) 128–137, http://dx.doi.org/10.1016/j.actaastro.2013.11.005.

[8] P. Huang, F. Zhang, J. Ma, Z. Meng, Z. Liu, Dynamics and configuration control of the maneuvering-net space robot system, Adv. Space Res. 55 (4) (2015) 1004–1014, http://dx.doi.org/10.1016/j.asr.2014.11.009.

[9] E.J. Van der Heide, M. Kruijff, Tethers and debris mitigation, Acta Astronaut. 48 (5–12) (2001) 503–516, http://dx.doi.org/10.1016/S0094-5765(01)00074-1.

[10] M.J. O'Connor, S. Clearly, D. Hayden, Debris de-tumbling and de-orbiting by elastic tether and wave-based control, in: 6th International Conference on Astrodynamics Tools and Techniques (ICATT), Darmstadt, Germany, 2016, p. 7.

[11] L.E.Z. Jasper, C.R. Seubert, H. Schaub, V. Trushlyakov, E. Yutkin, Tethered tug for large low earth orbit debris removal, in: Advances in the Astronautical Sciences, Vol. 143, Charleston, 2012, pp. 2223–2242.

[12] R. Dudziak, S. Tuttle, S. Barraclough, Harpoon technology development for the active removal of space debris, Adv. Space Res. 56 (3) (2015) 509–527, http://dx.doi.org/10.1016/j.asr.2015.04.012.

[13] O.G. Lagno, T.I. Lipatnikova, Y.N. Makarov, T.V. Mironova, V.I. Trushlyakov, Y.T. Shatrov, V.V. Yudintsev, Parameters design of autonomous docking module and the choice of suitable target and primary payload for ADR, in: T. Flohrer, F. Schmitz (Eds.), Proceedings of the 7th European Conference on Space Debris ESOC 18 - 21 April 2017, Vol. 7, ESA Space Debris Office, Darmstadt, Germany, 2017.

[14] V.I. Trushlyakov, V.V. Yudintsev, Rotary space tether system for active debris removal, J. Guid. Control Dyn. 43 (2) (2020) 354–364, http://dx.doi.org/10.2514/1.G004615.

[15] P. Tadini, U. Tancredi, M. Grassi, L. Anselmo, C. Pardini, A. Francesconi, F. Branz, F. Maggi, M. Lavagna, L.T. Deluca, N. Viola, S. Chiesa, V.I. Trushlyakov, T. Shimada, Active debris multi-removal mission concept based on hybrid propulsion, Acta Astronaut. 103 (2014) 26–35, http://dx.doi.org/10.1016/j.actaastro.2014.06.027.

[16] V.I. Trushlyakov, V.V. Yudintsev, Control of the rotating tethered system for orbital debris removal, in: Global Space Exploration Conference (GLEX2021), Paper Id GLEX-2021,7,5,6,X62094, International Astronautical Federation, IAF, St Petersburg, Russian Federation, 14-18 June 2021, 2021, URL: https://iafastro.directory/iac/paper/id/62094/summary/.

[17] K.T. Alfriend, S.R. Vadali, P. Gurfil, J.P. How, L.S. Breger, Rotation-translation coupling, 2010, http://dx.doi.org/10.1016/B978-0-7506-8533-7.00214-1.

[18] V.A. Chobotov, Orbital Mechanics, third ed., American Institute of Aeronautics and Astronautics, Reston, VA, 2002, pp. 45–152, http://dx.doi.org/10.2514/4.862250.

[19] R.R. Bate, D.D. Mueller, J.E. White, Fundamentals of Astrodynamics, Dover Publications, Inc., Mineola ,NY, 1971, pp. 419–425.